ELECTRICAL PROPERTIES OF PHOSPHOLIPID VESICLES

H. P. SCHWAN, S. TAKASHIMA, V. K. MIYAMOTO, *and* W. STOECKENIUS

From the Electromedical Division, The Moore School of Electrical Engineering, University of Pennsylvania, Philadelphia 19104 and the Cardiovascular Research Institute, University of California, San Francisco, California 94102

ABSTRACT The capacitance of the membrane of phospholipid vesicles and the electrical properties of the vesicle interior have been determined. To this end the electrical properties of phospholipid vesicles have been investigated over a frequency range extending from 1 kHz to 100 MHz. The dielectric behavior is characterized by two dispersions, one placed between 1 kHz and 1 MHz and the other between 1 and 100 MHz. The relaxational behavior at low frequencies is explained by counterion movement tangential to the vesicle surface and a reasonable value for the fixed charge of the vesicles is calculated from the dispersion magnitude. The relaxation at high frequencies is of the Maxwell-Wagner type and appears caused by the phospholipid bilayer bounding the interior phase of the vesicles. It is consistent with the existence of a closed bilayer with a capacitance of about 2 $\mu F/cm^2$ and an internal phase similar to the vesicle suspending medium. There is no indication of other than normally structured water inside the small vesicles.

INTRODUCTION

The physical properties of lipid bilayers are of interest because such bilayers may form the structural basis for all membranes (for review, see reference 1). In recent years, considerable progress has been made in the construction of model systems containing such bilayers in a form that allows experimental determination of electrical parameters and permeability. We have developed such a system, described in more detail elsewhere (references 2 and 3 and footnote 1), which consists of a suspension of vesicles bounded by one bilayer of phospholipids. This report describes the electrical impedance of the system. It shows that the bilayer forms a closed surface. The bilayer capacitance and the electrical properties of the vesicle interior have been determined.

The electrical capacitance of a suspension of cellular particles is a direct measure of the suspension's content of completely membrane-enclosed particles. This may be seen as follows.

[1] Miyamoto, V. K., and W. Stoeckenius. Manuscript in preparation.

The low frequency dielectric constant ϵ_0 of a suspension of cells is given by Schwan, 1957, p. 162 (4):[2]

$$\epsilon_0 = \epsilon_\infty + \frac{9}{4\epsilon_r} \frac{pRC_m}{[1 + RG_m(\rho_i + 0.5\rho_a)]^2}, \quad (1)$$

where ϵ_r is the dielectric constant of free space, p is the volume fraction taken by the cells, C_m is the capacitance per cm² surface of the membrane, G_m is the conductance per cm² membrane surface, R is the cellular radius, and ρ_i, ρ_a is the resistivity of cell interior and suspending medium and where ϵ_∞ is a contribution from mechanisms other than those due to membrane polarization.

ϵ_∞ is usually observed at high frequencies and is not too different from the dielectric constant of suspending medium. Thus, for a volume fraction $p = 0.3$, a membrane capacitance of $C_m = 1$ μF/cm², a membrane conductance which is small enough not to affect Equation 1, and a radius of $R = 0.1$ μ, $\epsilon_0 - \epsilon_\infty = 80$. In the case that all the cells are broken into fragments, the dielectric constant ϵ_0 is obtained by weighted averaging of the dielectric constants of suspending and suspended phases. A membrane capacitance of 1 μF/cm² is typical of the existence of 100-A-thick membranes of a dielectric constant 10, and the assumed values of p and R correspond to a membrane volume fraction $p_m = 0.1$. Hence, the membrane fragments reduce the dielectric constant of the suspending phase (near 80) by a small amount. This demonstrates that, while membrane fragments decrease the dielectric constant of the suspending phase, membranes which completely surround cells, increase it.

Typical membrane conductance values G_m range from 1 to 100 mmho/cm². For typical cell radii in the μ range and less, the expression in Equation 1, $RG_m(\rho_i + 0.5\ \rho_a)$ is therefore very small compared to unity and, hence, G_m does not affect C_m.

Typical C_m values range somewhere between 0.6 and 1.5 μF/cm², i.e., are close to 1 μF/cm². This value of 1 μF/cm² can be considered to represent either the presence of a 30- or 40-A-thick bilayer membrane whose material has a typically low dielectric constant of 3 or 4 or the presence of a membrane of some 100 A of dielectric constant near 10. While thickness values near 100 A are typical for biological membranes, we have pointed out that their capacitance nevertheless can originate from an inner bilayer lipid film (reference 4, p. 164, and reference 5, p. 402). It is reasonable to assume that the bilayers of interest in this study have a capacitance of the same order of magnitude and we shall see that the evaluation of the measured data is consistent with this.

Equations which state the frequency dependence of the dielectric constant ϵ and conductivity κ of closed vesicles are derived in Appendexes I and II. They permit a comparison of observed data with the behavior calculated if one assumes closed vesicles. They also permit reduction of measured bulk values to bilayer capacitance.

As the frequency of the applied field is increased the bilayers are eventually short circuited. As a consequence, both dielectric constant ϵ and conductivity κ change with frequency in accordance with Equations 12 and 13 in Appendix I. It is also ap-

[2] Equation 1 applies if the membrane thickness is very small in comparison to the cell radius R and if the volume fraction p is small. Equations which are not based on these two assumptions, but assume $G_m = 0$ instead, are derived in Appendix I.

parent from Equations 12 *a* and 13 *a* in Appendix I that the conductivity change with frequency is the more pronounced the smaller the time constants, which characterize the frequency range where the changes of ϵ and κ take place. Model calculations using reasonable parameters and using the equations given in Appendix I indicate that the dielectric sonstant change should be between 10 and 30 units and takes place in the frequency range near 10 MHz.

It is to be anticipated that the bilayers under consideration carry fixed charges arising from the orientation of polar molecular groups at the membrane surfaces. In the presence of such fixed charges relaxation of the counterions occurs. Experimental evidence and the theory for counterion relaxation have been presented by Schwan, Schwarz, Maczuk, and Pauly (6) and Schwarz (7). Time-constant T and dielectric increment $\Delta\epsilon$ are given by the equations

$$T = \frac{R^2}{2\mu k T_0} \tag{2}$$

$$\Delta\epsilon = \frac{9}{4} \frac{p}{\left(1 + \frac{p}{2}\right)^2} \frac{e_0^2 R\sigma}{\epsilon_r k T_0}, \tag{3}$$

where R is the radius of particle, to be large compared to the thickness of the double layer, μ is the counterion mobility, κ is the Boltzmann constant, T_0 is the absolute temperature, p is the volume fraction occupied by particles, e_0 is the elementary charge, and σ is the counterion surface density (ions/unit area), and provided that the individual particle does not contribute noticeably to its total induced dipole moment, i.e., that its effective dielectric constant is negligible.

For typical mobilities μ, characteristic frequencies $f_c = \frac{1}{2}\pi T$ are about 0.1 kHz for a radius of $R = 1\ \mu$ and 1 MHz for 100 A. Increments may range from 10^4 to 10^5 and 10^2 to 10^3, respectively, for reasonable ϵ_0 and σ values and p values near 0.3.

It appears therefore that bilayer-enclosed particles of a diameter of about 0.1 μ or less should display two frequency dependencies of the relaxational type: one occurring at frequencies below 1 MHz which is distinguished by a large dielectric increment and caused by counterions relaxing about the charged surface of the closed cell; and a second one, occurring somewhere near 10 MHz, as may be judged from model calculations using the equations in Appendix I. The second is characterized by a smaller dielectric increment but a much larger conductance change and consistent with the existence of a closed vesicle surface. This is precisely the behavior observed.

MATERIAL

The vesicle suspension was prepared by homogenization, sonication, centrifugation, and dialysis of a 10% lipid buffer mixture (mass:volume). The lipid was Asolectin (Associated Concentrates, Woodside, L. I., N. Y.), a complex mixture of primarily phospholipids derived

from soybean. Asolectin is roughly 70% phospholipid by mass, assuming the average phospholipid phosphorus content of 4%. This lipid mixture was used to explore the techniques for studying vesicles because it is inexpensive and readily available. The pH of the buffer was adjusted to 7.1 at 23°C by addition of hydrochloric acid. The buffer was 0.25 M in sucrose, 0.0005 M disodium EDTA, 0.0075 M in α-thioglycerol and 0.01 M in tris(hydroxymethyl)-aminomethane.

The size distribution of the preparation was measured by electron microscopy of thin sections of osmium-fixed vesicles. Corrections were applied for section thickness.

The following samples were investigated.

(*a*) One sample at 12°C. Volume fraction of vesicles $p = 0.14$.

(*b*) Samples of volume fraction $p = 0.14$, 0.07, 0.035, and 0.0175. This dilution experiment was carried out to check the linearity of dielectric increments with p demanded by theory. Temperature 9°C.

(*c*) One sample, $p = 0.07$, at 9°C, 20°C, and 30°C. The dielectric behavior was observed to change with temperature in accordance with theoretical anticipation.

(*d*) One sample, $p = 0.07$, at 5°C.

Solid weight percentages were determined from analysis of lipid phosphorous (8). Lipids in suspension were extracted by the Folch technique (9) and were found to contain 3.09% phosphorus.

Cell radius R and membrane thickness d were obtained from electronmicroscopy and typically $R = 135$ A and $d = 35$–45 A. Particle size variation appears small enough to justify for the present purposes a model based on only one size (see for example reference 10).[3] Cellular vesicle volume fractions p were determined from the volume taken by the solids using

$$v/p = 1 - a, \tag{4}$$

where $a = (1 - d/R)^3$ is the volume fraction taken by the interior of the vesicle. Bilayer volume fraction values v are obtained from solid weight percentages and specific weight of the lipid constituents, and compare with values obtained from dielectric decrements at high frequencies, using reference 4, pp. 192, 199.

$$\Delta\epsilon = \epsilon_a - \epsilon = 120v. \tag{5}$$

ϵ of the suspending phase is close to that of water and 82 for 12°C. The numerical factor of 1.2 is based on investigations of a broad spectrum of cellular structures, including erythrocytes, bacteria, PPLO, and various tissues.[4] v estimates are accurate to about 20% relative.

p values calculated from v are based on the assumption of uniform vesicle size. However a distribution of size will permit the larger vesicles to contribute per gram lipid more strongly to p than the smaller ones. Hence, the volume concentration calculated assuming uniform vesicle size is probably somewhat too small (see Table I). Fortunately the membrane capacitance values C_m and internal conductivity κ_i turn out to be fairly insensitive to p. p values

[3] More than three-quarters of all particles are contained within the radial range from 100 to 200 A.

[4] The dielectric decrement is caused by the macromolecular content of the cells investigated. The numerical factor is obtained at frequencies where polarization of the macromolecules either due to side chain rotation or relaxation of bound water can be neglected. It should apply whenever the dielectric constant of the solid is small in comparison to that of the electrolyte, and hence, is anticipated to be applicable in the present case. Its value is readily derived from Equation 1 in Appendix II, if the κ's are replaced by ϵ's at high frequencies.

TABLE I

LIMIT VALUES ϵ_0 AND ϵ_∞ OF DIELECTRIC CONSTANT

$\epsilon_{0\beta}$ is calculated from ϵ_∞ and $\Delta\epsilon(\beta)$, $\Delta\epsilon(\alpha)$ from ϵ_0 and $\epsilon_{0\beta}$. The $\Delta\epsilon(\beta)$ values are obtained from conductance dispersion and $f(\beta)$ (approach I) and from the dielectric increment $\epsilon_{0\beta} - \epsilon_\infty$ and $f(\beta)$ (approach II). The values indicated by ? are rather uncertain owing to the small magnitude of the β dispersion. Variation of temperature (sample 3) appears not to affect $\Delta\epsilon(\beta)$ greatly. p values for samples 1–3 calculated from ν. The two values of sample 4 are calculated from ν and evaluated from size distribution.

	ϵ_0	ϵ_∞	$\epsilon_{\infty\alpha} = \epsilon_{0\beta}$	$f(\alpha)$	$\Delta\epsilon(\alpha)$	$f(\beta)$	I $\Delta\epsilon(\beta)$	II $\Delta\epsilon(\beta)$
				kHz		*MHz*		
Sample 1 (12°C; $p = 0.14$)	355	72	90	45	285	9	18	20
Sample 2 (9°C)								
$p = 0.14$		72	90			10	23	12
0.07	250	78	90	40	160	20	13	10
0.035	180	80	88	30	92	25	9	6
0.035	215			12 (?)				
0.017	140	82	89	18	51	40 (?)	5 (?)	4 (?)
Sample 3 $p = 0.07$;								
9°C		78				20	13	8
20°C		76				20	12	8
30°C		72				30	11	7
Sample 4 (5°C, $p = 0.05$ 0.078)	300	81	93	20	207	6	13	10

are judged to be accurate to 30% relative, with a tendency towards low values, if calculated from p assuming uniform radius R.

MEASUREMENTS

Measurements of dielectric constant ϵ and conductivity κ were carried out over the frequency range from 100 Hz to 100 MHz. From 0.1 to 200 kHz a low frequency bridge developed for the study of the dielectric properties of biological material was used (11, 12). The sample cell of cylindrical cross-section and variable electrode distance has been described elsewhere (reference 12, Fig. 23). The electrode distance was varied and the platinum electrodes covered with a heavy coat of platinum black in order to reduce the effects of electrode polarization (reference 12, p. 340). Drift of the sample properties was minimized by choice of a low temperature, and by the application of a correction technique employing repeated measurements at a reference frequency (reference 12, p. 369).

A Boonton Radio Corporation (Hewlett-Packard) RX-meter, type 250-A, was used for the frequency range extending from 0.5 to 100 MHz, using a sample cell also described before (reference 12, Fig. 37 *a*). Problems of drift and electrode polarization were not disturbing above 0.5 MHz. Evaluation of sample properties was carried out with due consideration of the effects of stray capacitances and lead inductances, using techniques which have

also been described before (12). The cell constant of the sample cell was determined at various frequencies with electrolytes of conductivities comparable to those of the sample. Accuracy of the Boonton instrument declines above 50 MHz and κ determinations at higher frequencies were accurate to 1% or 2% (see Fig. 2).

RESULTS

Figs. 1 and 2 demonstrate the results obtained with sample 1, Table I, part of those obtained with all series. They demonstrate the existence of two dispersions. One termed α dispersion, occurs at low frequencies and is characterized by a large change in dielectric constant. The second, labeled β, displays a strong change in conductance and occurs at high frequencies. Limit values of α and β dispersion $\epsilon_{0\alpha}$ and $\epsilon_{\infty\beta}$ are immediately apparent. So are average characteristic frequencies $f(\alpha)$ and $f(\beta)$ where ϵ of the α dispersion and κ of the β dispersion reach values halfway between respective limit values.

ϵ_0 values of the β dispersion $\epsilon_{0\beta}$ are difficult to obtain since the high frequency runout of the α dispersion prevents a plateau between α and β dispersion. In order to

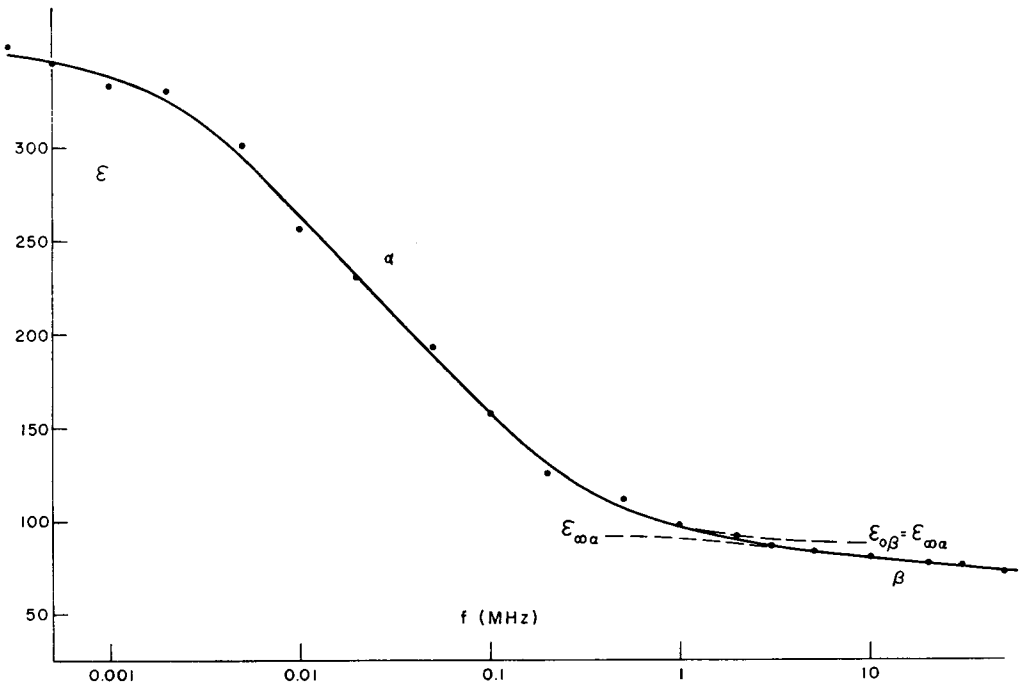

FIGURE 1 Dielectric constant ϵ as function of frequency. Two relaxational processes labeled α and β are indicated. The β process is inferred by a comparison with data obtained on polystyrene latex (6, 7). In the absence of the β dispersion, the α process should more rapidly approach its limit value towards higher frequencies as indicated by the dashed extension of the α dispersion.

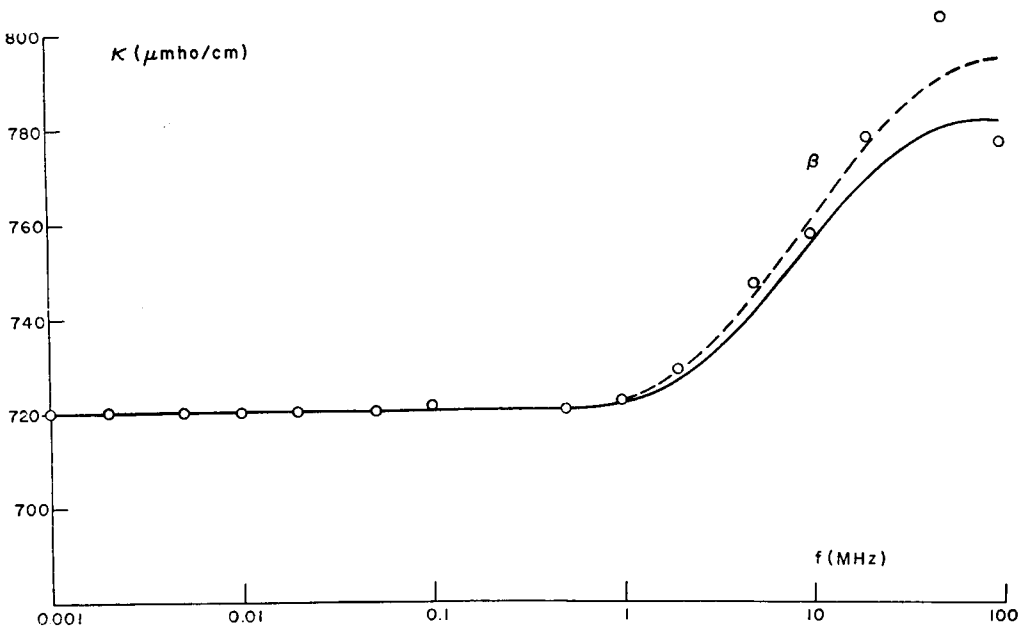

FIGURE 2 Conductivity κ as function of frequency. The β dispersion is clearly noticeable, while the α dispersion is not recognizable with the chosen ordinate scale. The solid curve is calculated from the data given in Table III.

aid the following techniques to determine $\epsilon_{0\beta}$, the following time constants are defined:

T_1, T_2 Time constants as defined by Equations 12 and 13 in Appendix I.

$T(\text{av})$ Mean of T_1 and T_2.

T^* Time constant determined from over-all ϵ- and κ-change, i.e., by equation

$$\kappa_\infty - \kappa_0 = (\epsilon_0 - \epsilon_\infty)\epsilon_r/T(\text{av}). \tag{6}$$

$T(\beta)$ Time constant defined by the characteristic frequency $f(\beta) = \frac{1}{2}\pi T(\beta)$ where the conductance is the mean of its two limit values at low and high frequencies.

T' Time constant defined by the characteristic frequency $f' = \frac{1}{2}\pi T'$ where the dielectric constant is the mean of its two limit values.

The characteristic frequencies f_1, f_2, f^*, $f(\beta)$, and f', if multiplied by 2π, are the inverse of the respective time constants. There is always a sequence

$$T_1 > T' > T^* > T(\beta) > T_2 \tag{7}$$

and hence,

$$f_1 < f' < f^* < f(\beta) < f_2, \tag{7a}$$

i.e., the time constants T', T^*, and $T(\beta)$ are contained within the interval between T_1 and T_2. This is readily apparent from a discussion of Equations 9 and 10 and demonstrated in Fig. 5.[5] In the case of interest to us, only $T(\beta) = \frac{1}{2}\pi f(\beta)$ is experimentally available.

The values for the magnitude $\epsilon_0 - \epsilon_\infty$ of the β dispersion may be estimated from the difference $\kappa_\infty - \kappa_0$ and Equation 6 using the time constant $T(\beta) = \frac{1}{2}\pi f(\beta)$ instead of $T(\text{av})$. $\epsilon_{0\beta}$ values can also be obtained from the dielectric constant observed at the average characteristic frequency $f(\beta)$ using the approximation

$$\epsilon(f_\beta) = \tfrac{1}{2}(\epsilon_0 + \epsilon_\infty), \tag{8}$$

even though $f(\beta)$ is obtained from the conductivity data and not from ϵ and Equation 8 strictly valid only if $f(\beta)$ is replaced by f'. The above outlined two estimates of $\epsilon_0 - \epsilon_\infty$ are the more accurate the less the difference between the two time constants T_1 and T_2. A study of the experimental data indicates that the two time constants are of the same order of magnitude. Model calculations support that with ratios of T_1 and T_2 smaller than three $\epsilon_0 - \epsilon_\infty$ values are provided by above outlined procedures which deviate from the true difference $\epsilon_0 - \epsilon_\infty$ by a ratio much less than two. It also follows from equations 7 and 7 *a* that the estimates for $\epsilon_0 - \epsilon_\infty$ are on the low side.

The magnitude of the β-dispersion $\Delta\epsilon_\beta = \epsilon_{0\beta} - \epsilon_\infty$ is given in Table I, using both approaches presented above. The results agree within a factor of two as anticipated. From the measured ϵ_∞ and the average of the two values for $\epsilon_{0\beta} - \epsilon_\infty$, $\epsilon_{\infty\alpha} = \epsilon_{0\beta}$ can be calculated, and from $\epsilon_{\infty\alpha}$ and ϵ_0 the magnitude of the α dispersion $\Delta\epsilon_\alpha$ is obtained. Since $\Delta\epsilon(\alpha)$ is much larger than $\Delta\epsilon(\beta)$, $\Delta\epsilon(\alpha)$ is rather insensitive to $\epsilon_{\infty\alpha}$.

DISCUSSION

Fig. 1 clearly indicates a very pronounced frequency dependence of ϵ at low frequencies and a less pronounced one at high frequencies above 1 MHz. Fig. 2 shows a complementary behavior of the conductivity κ as required by the approximate equation

$$\kappa_\infty - \kappa_0 = (\epsilon_0 - \epsilon_\infty)\epsilon_r/T. \tag{9}$$

Equation 9 applies to both low frequency and high frequency data individually and is approximately valid for dielectric dispersions characterized by narrow to moderately broad spectra of time constants and, hence, not unexpected. The strong α

[5] Analysis of the data of sample 1 provides

$$f_1 = 5.7; \quad f^* = 6.7; \quad f(\beta) = 8; \quad f_2 = 19.4 \text{ MHz}.$$

The time constant $T(\text{av})$ as defined by Equation 18 *a* in Appendix I corresponds to $f(\text{av}) = 8.6$ MHz. It agrees well with $f(\beta)$.

dispersion of ϵ at low frequencies represents counterion relaxation about the closed bilayer surface. The strong β dispersion of κ at high frequencies is anticipated from the Maxwell-Wagner model of membrane-bounded spherical particles treated in Appendix I. It cannot be explained by a suspension of solid lipid particles since the dispersion magnitude for such a system is only about 1 % of that observed. This may be seen from an appropriate use of Equation 1 in Appendix II.

α Dispersion

Equation 3 predicts that the dielectric increment of the α dispersion $\Delta\epsilon(\alpha)$ should be proportional to the size of the particle and particle concentration. Particle concentration proportionality is indicated by all data as demonstrated in Fig. 3. Results

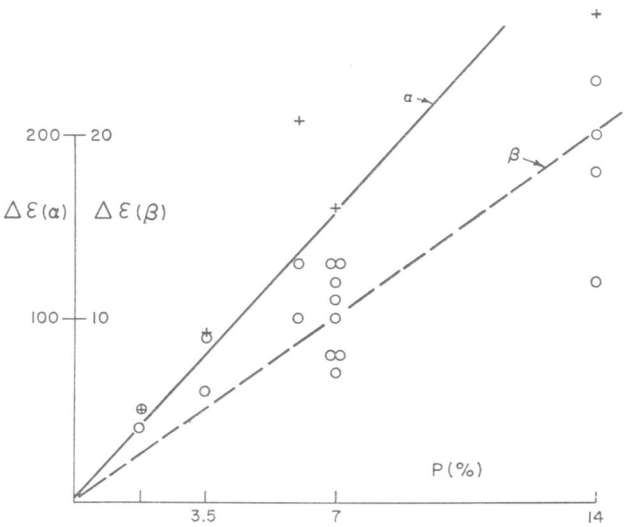

FIGURE 3 Magnitude of α and β dispersion as function of vesicle volume fraction p (expressed in percentage of total volume).

previously obtained on polystyrene particles (6) are compared with those obtained in this study in Table II. Deviations from exact proportionality reflect most likely some variation in charge density σ. It is of particular interest to compare the surface charge obtained from Equation 3 with microelectrophoretic determinations (4).[6] This was done in one case (sample 4) for a volume fraction of $p = 6\%$ yielding a $\Delta\epsilon(\alpha) = 210$ at a temperature of 5°C. The value obtained from $\Delta\epsilon(\alpha)$ is 6.10^{-16} coulomb/vesicle while that from electrophoresis is 5.10^{-16} coulomb/vesicle for the same material. The values agree within experimental limits, supporting the conclusion that the α dispersion is counterion induced.

The characteristic frequency of the α dispersion is given by Equation 2 and re-

[6] Mel, H. C. Personal communication.

TABLE II

MAGNITUDE OF DIELECTRIC DISPERSION AS FUNCTION OF PARTICLE DIAMETER

Deviations from linearity between $\Delta\epsilon$ and $2R$ are largely due to variation in surface charge density. All values adjusted to a volume concentration near 15%.

	$2R(\mu)$	$\Delta\epsilon(\alpha)$
Polystyrene	1.2	5000
"	0.6	1500
"	0.2	1200
"	0.09	250
Lipid vesicles	0.025	250

ported to be 80 kHz at 25°C for polystyrene particles in KCl and a diameter of 880 A (6). Equation 2 would predict about 400 kHz for the particles of present interest, with due corrections for temperature difference and different mobility of KCl and NaCl. This is much higher than the value of 45 kHz taken from Fig. 1. The values obtained from the sample series 2 and 3 were even lower, ranging from 12 to 40 kHz, reflecting in some cases uncertainty in the precise value of ϵ_0. The theory on which Equation 2 is based assumes particles of low effective dielectric constant. This assumption does not apply in our case, which may explain the difference between experimental and theoretical T values. Another explanation is suggested by the fact that Equation 3 fared rather well, while Equation 2 failed. Only Equation 2 contains the counterion mobility μ, suggesting that it is considerably lower in the case at hand than that of "free" ions. This may well reflect noticeable electrostatic interaction with the fixed charges.

β Dispersion

The high frequency behavior permits the determination of the bilayer capacitance C_m. Its determination and that of other quantities of interest proceeds as follows:

(a) κ_a is calculated from κ_0, using Equation 19 in Appendix I.

(*b*) From $\epsilon_{0\beta} = \epsilon_0$ the bilayer capacitance value of C_m is calculated using Equation 21 in Appendix I.

(*c*) From C_m and bilayer thickness, the bilayer dielectric constant ϵ_m can be calculated.

(*d*) From C_m, κ_a and the average characteristic frequency $f^* = \frac{1}{2}\pi T^*$ of the β dispersion κ_i is calculated using Equation 23.

(*e*) From ϵ_∞, the value of ϵ_m can be estimated, using Appendix II equations, and can be compared with that obtained as stated under (*c*).

(*f*) With the information now at hand, conductivity values are calculated and compared with the experimental κ values. The calculated curve may be used to again go through the total procedure, including determination of T and ϵ_0 from κ. How-

ever iteration is unnecessary since calculated and experimental data are essentially identical.

The magnitude of the β dispersion is plotted against p in Fig. 3. $\epsilon_{0\beta} - \epsilon_\infty$ appears proportional to p as it should be since the first term of Equation 20 in Appendix I changes but little with p. The scatter of the data demonstrates the low accuracy of $\epsilon_{0\beta} - \epsilon_\infty$ and p.

In Fig. 4 the decrement $\epsilon_{H_2O} - \epsilon_\infty$ is plotted against p. The solid lines are predictions for $\epsilon_m = 3$ and $\epsilon_m = 11$, using Equation 7 in Appendix II. The experimental data appear to favor a value ϵ_m nearer 10, lower than that derived from C_m. The data scatter is considerable, reflecting an accuracy of ϵ of near one dielectric unit. For sample 1 the following data are obtained.

	$p = 0.14$:	$p = 0.20$:[7]
C_m	7.7 μF/cm^2	7.2 μF/cm^2
ϵ_m	37	33
η_i/η_a (assuming $\epsilon_i = \epsilon_a$)[8]	0.9	0.7

The coefficients A–F, time constants, and dispersion parameter derived from these values are presented in Table III. It is of particular interest that the magnitude of the dispersion 2 establishes a rather small contribution to the β dispersion. The solid curve in Fig. 2 is calculated using these results and the equations in Appendix I. It agrees with the experimental data. It is apparent from Table I and Figs. 3 and 4 that the data obtained with other samples are in line with these results.

The bilayer capacity of about 7 μF/cm^2 is about double as high as that of most biological membranes. The value of 7 μF/cm^2 corresponds for a bilayer thickness of 42 A to a dielectric constant near 30 while biological membranes, with a thickness near or somewhat above 100 A have a dielectric constant near 10. A rationale for the high dielectric constant of biological membranes has been given (4, 5). It possibly is due to the series combination of 30 A lipid layer of low dielectric constant with two layers of similar thickness and high dielectric constant. A similar model cannot yet be proposed for the vesicle bilayer. If one would assume a bilayer thickness of only 30 A, representing an inner hydrocarbon layer of a dielectric constant of 5, and assume that the other 12 A are of high dielectric constant since they contain much water, then a total capacitance C_m near 2 μF/cm^2 would be anticipated and the dielectric constant would be near 7. However, if one would mix one-third hydrated macromolecules of high dielectric constant (13, 14) with two-thirds lipid matter in a less ordered random way, a dielectric constant near 30 could result.

[7] The higher p value is chosen to illustrate how the increase in p effects C_m, ϵ_m and κ_i. Clearly, a variation in p by about 50% upwards does not noticeably effect C_m and ϵ_m.

[8] The dielectric constant of free water and that bound to macromolecules such as hemoglobin and albumin appear of similar magnitude (13, 14). At that, a very low ϵ_i would lower κ_i by only one third.

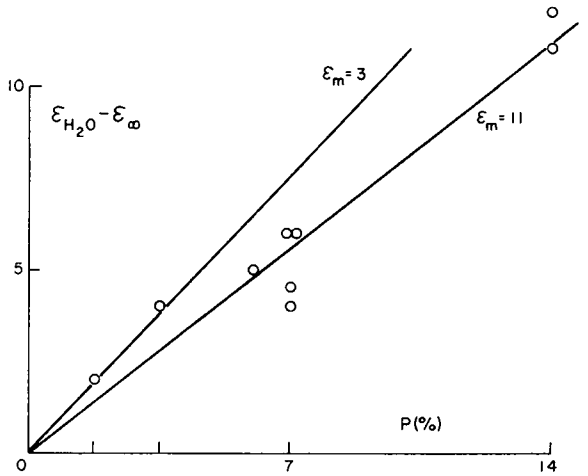

FIGURE 4 Magnitude of the high frequency limit decrement $\epsilon_{H_2O} - \epsilon_\infty$ as function of p. The two solid lines are calculated assuming a membrane dielectric constant of 3 and 11, respectively.

TABLE III

PARAMETERS FOR SAMPLE 1

The data are typical for all data of similar volume concentration ($p = 0.14$).

$A = 1.01\ \kappa_a^2$	$T_1 = 1.57\ \epsilon_r \cdot 183/\kappa_a$
$B = 26{,}500\ \epsilon_r^2$	$T_2 = 0.43\ \epsilon_r \cdot 183/\kappa_a$
$C = 1.29\ \kappa_a^2$	$f_1 = 3.8$ MHz
$D = 29{,}500\ \epsilon_r^2$	$f_2 = 14$ MHz
$E = 417\ \kappa_a \epsilon_r$	$\Delta\epsilon_1 = 15.5$
$F = 472\ \kappa_a \epsilon_r$	$\Delta\epsilon_2 = 1$
	$\Delta\kappa_1 = 49\ \mu$mho/cm
	$\Delta\kappa_2 = 11\ \mu$mho/cm

Thus, the molecular arrangement is demonstrated to have a rather decisive influence on the dielectric constant.

We wish to emphasize that the magnitude of the β dispersion could be only crudely estimated and there is not necessarily a contradiction between the ϵ_m values of 10 and 30 obtained from ϵ_∞ and C_m. However it is difficult to see how a dielectric constant of only a few dielectric units could be made consistent with the data reported above. For a detailed analysis of the large uncertainties, see Oldenburg (15).

Of particular significance are the values for the internal conductivity κ_i. The difference of some 10% or 30% between κ_i and κ_a is well within the range of error. There is however no doubt that κ_i and κ_a are of comparable magnitude. The agreement of the κ values in and outside the membranes appears to suggest that water in-

side small vesicles such as investigated here is not structured, or "bound," to such an extent as to inhibit ionic mobility. This conclusion does not necessarily conflict with our previous work on the properties of protein bound water (13, 14). This work indicated structured water reaching out up to about 10 A from the macro-molecular surface. If such structured water were adjacent to the interior of the vesicle membrane, it would only occupy a minor fraction of the total vesicle interior. Similarly, the studies on electrical properties of the erythrocyte interior reported by Pauly and Schwan (16) are in no conflict, since this work indicated deviation between anticipated and observed conductance values inside the cells only for high Hb content and the vesicles contain no proteins inside.

In conclusion then, it can be stated that the dielectric study of the vesicle suspension indicates the following features:

(*a*) At low frequencies the suspension undergoes a counterion-induced relaxation. The surface charge calculated from the magnitude of this dispersion compares well with electrophoretic data.

(*b*) At high frequencies a Maxwell-Wagner dispersion whose magnitude is small in ϵ but definitely noticeable in κ, exists. It is characterized by two time constants, even though the relaxation characterized by the smaller of the two contributes but little to the total dispersion. The dispersion indicates a bilayer dielectric constant near or higher than 10. Ionic mobility and concentration inside the vesicles appear comparable to outside values and, thus, the water inside is not of the "bound" type.

We appreciate Dr. M. Eigen's interest in this work.

This work was supported by Program Project Grant HE-06285 and Graduate Training Grant HE-5251 from the National Heart and Lung Institute and by the United States Public Health Service Grant Number HE-01253-18.

Part of this work was carried out while one of us (Schwan) visited the Max Planck Institut fur Physikalische Chemie, Goettingen, Germany.

Received for publication 19 May 1970.

APPENDIX I

Expressions for the specific admittance $K = \kappa + j\omega\epsilon\epsilon_r$ of a suspension of membrane-bounded cells (Fig. 5) have been frequently cited in the literature. However, almost all of these expressions assume that the volume occupied by the cell membrane is vanishingly small in comparison to that of the cell itself. In order to derive equations which are suitable in any case we proceed as follows. Pauly and Schwan (Equation 12, reference 17) as well as Schwan and Morowitz (Equation 3, reference 5) state

$$\frac{K}{K_a} = \frac{A - B\omega^2 + jE\omega}{C - D\omega^2 + jF\omega}, \qquad \text{(AI 1)}$$

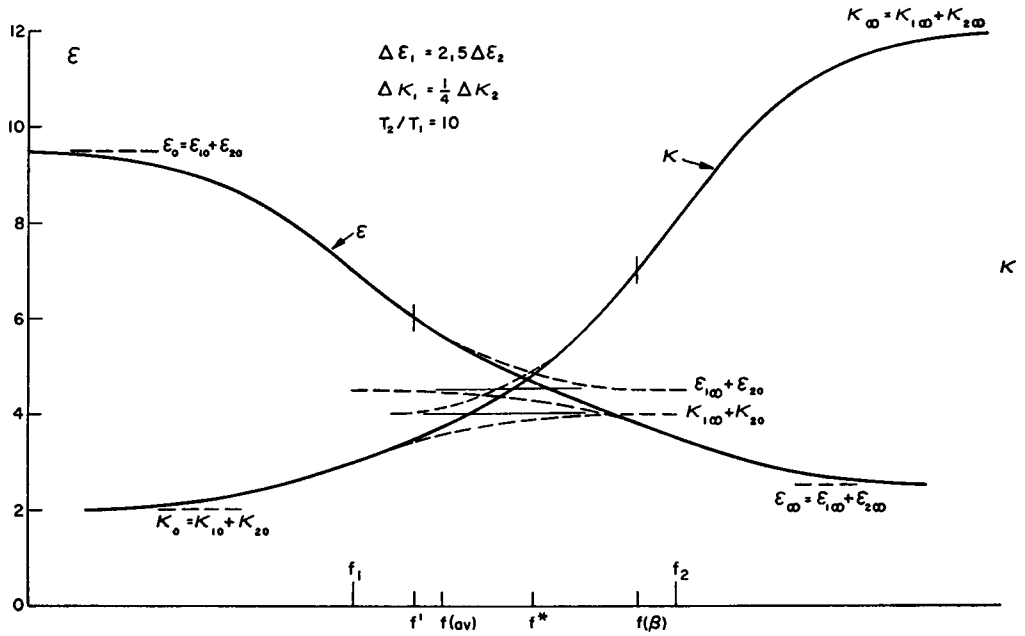

FIGURE 5 An example illustrating the dielectric behavior in the presence of two time constants T_1 and T_2. Even though the time constant ratio was chosen as high as 10, the two dispersions characterized by T_1 and T_2 are overlapping to such an extent that separation from experimental data is difficult.

where, from Equations 12–14, appendix of reference 5

$$A = 2(1 - p)\kappa_a\kappa_i' \tag{AI 2}$$

$$B = RC_m'\epsilon_r[(1 + 2p)\epsilon_i' + 2(1 - p)\epsilon_a] + 2(1 - p)\epsilon_a\epsilon_i'\epsilon_r^2 \tag{AI 3}$$

$$C = (2 + p)\kappa_a\kappa_i' \tag{AI 4}$$

$$D = RC_m'\epsilon_r[(1 - p)\epsilon_i' + (2 + p)\epsilon_a] + (2 + p)\epsilon_a\epsilon_i'\epsilon_r^2 \tag{AI 5}$$

$$E = RC_m'[(1 + 2p)\kappa_i' + 2(1 - p)\kappa_a] + 2\epsilon_r(1 - p)(\kappa_a\epsilon_i' + \kappa_i'\epsilon_a) \tag{AI 6}$$

$$F = RC_m'[(1 - p)\kappa_i' + (2 + p)\kappa_a] + \epsilon_r(2 + p)(\kappa_a\epsilon_i' + \kappa_i'\epsilon_a) \tag{AI 7}$$

with

$$\kappa_i' = \frac{1 - 2\Delta/R}{1 - \Delta/R}\kappa_i \sim \kappa_i(1 - d/R) \tag{AI 8}$$

$$\epsilon_i' = \frac{1 - 2\Delta/R}{1 - \Delta/R}\epsilon_i \sim \epsilon_i(1 - d/R) \tag{AI 9}$$

$$C_m' = C_m \frac{d}{D} \frac{1 + 2a}{1 - a}, \qquad \text{(AI 10)}^9$$

where a is the relative cell volume fraction occupied by the cell interior and where the quantity Δ is defined by

$$a = (1 - d/R)^3 = 1 - 3\Delta/R; \qquad \text{(AI 11)}$$

and where C_m is the membrane capacitance per cm², R is the cell radius, d is the membrane thickness, κ is the electrical conductivity = 1/specific resistance ρ, ϵ is the dielectric constant relative to free space, ϵ_r is the dielectric constant of free space, 8.84×10^{-14} F/cm, and i, a are subscripts denoting interior of cell and suspending medium.

The equations AI 2–AI 7 are simpler than equations given by Pauly and Schwan (16) and, hence, are used here. However, the following assumptions, fulfilled in the present case, must be made in order to arrive at the above equations (see reference 5).[10]

Assumption a. $|K_m| < (1/3)|K_i|$, where K_m and K_i are the specific admittances of membrane material and cell interior.

Assumption b. $\kappa_m = 0$, i.e., the membrane conductance is so small that it does not affect the admittance of the cell suspension.

Equation AI 1 can be separated into two equations (reference 16), each containing in turn two relaxation expressions of the Debye type:

$$\kappa = \frac{\kappa_{10} + \kappa_{1\infty}(\omega T_1)^2}{1 + (\omega T_1)^2} + \frac{\kappa_{20} + \kappa_{2\infty}(\omega T_2)^2}{1 + (\omega T_2)^2} \qquad \text{(AI 12)}$$

$$\epsilon = \frac{\epsilon_{10} + \epsilon_{1\infty}(\omega T_1)^2}{1 + (\omega T_1)^2} + \frac{\epsilon_{20} + \epsilon_{2\infty}(\omega T_2)^2}{1 + (\omega T_2)^2}. \qquad \text{(AI 13)}$$

The parameters are limit values at frequencies which are low and high in comparison to the "characteristic frequencies" $\frac{1}{2}\pi T_1$ and $\frac{1}{2}\pi T_2$ of the individual relaxation terms. They are interrelated by (see for example, reference 4)

$$\kappa_{1\infty} - \kappa_{10} = \frac{1}{T_1}(\epsilon_{10} - \epsilon_{1\infty})\epsilon_r \qquad \text{(AI 12}a\text{)}$$

$$\kappa_{2\infty} - \kappa_{20} = \frac{1}{T_2}(\epsilon_{20} - \epsilon_{2\infty})\epsilon_r. \qquad \text{(AI 13}a\text{)}$$

An illustration of the frequency dependance of ϵ and κ is presented in Fig. 4. Over-all limit values of dielectric constant and conductivity for low and high frequency may be indicated by subscripts 0 and ∞. They are, from Equations 21–23 and 26 of reference 16:

[9] Equation 10 in the Appendix of reference 3 should contain $1 - 2\Delta/R$ in the numerator instead of the denominator.

[10] Assumption a is fulfilled if $\epsilon_m < (1/3)\epsilon_i$ and $\kappa_m < (1/3)\kappa_i$. The dielectric constant ϵ_m is likely to be somewhere between 3 and 10 (see for example reference 2) while that of ϵ_i is close to 80, i.e., about 10 times larger. The conductance requirement is met by assumption b. Assumption b is inherent in the chosen model, where a membrane conductance of sufficient magnitude to effect ϵ was ruled out.

$$\kappa_0 = \kappa_a \frac{A}{C} \tag{AI 14}$$

$$\kappa_\infty = \frac{1}{D^2}[\kappa_a BD - \epsilon_r \epsilon_a (BF - DE)] \tag{AI 15}$$

$$\epsilon_0 = \frac{1}{\epsilon_r C^2}[\epsilon_r \epsilon_a AC - \kappa_a (AF - EC)] \tag{AI 16}$$

$$\epsilon_\infty = \epsilon_a \frac{B}{D}. \tag{AI 17}$$

The two time constants T_1 and T_2 are

$$T_{1,2} = \frac{F}{2C}\left[1 \pm \sqrt{1 - \frac{4DC}{F^2}}\right] \tag{AI 18}$$

and the average of the time constants T_1 and T_2

$$T_{av} = \frac{1}{2}(T_1 + T_2) = \frac{F}{2C}. \tag{AI 18 a}$$

Introduction of Equations AI 2–AI 7 into Equations AI 14–AI 18 results in the simple expressions

$$\kappa_0 = \kappa_a \frac{1 - p}{1 + p/2} \tag{AI 19}$$

$$\kappa_\infty = \kappa_a \frac{B}{D} - \frac{\epsilon_r^2 \epsilon_a}{D^2} 9pRC_m'[\epsilon_r \epsilon_i'^2 \kappa_a + RC_m'^2(\epsilon_i' \kappa_a - \kappa_i' \epsilon_a)] \tag{AI 20}$$

$$\epsilon_0 = \epsilon_a \frac{1 - p}{1 + p/2} + \frac{9}{4} \frac{p}{(1 + p/2)^2} \frac{RC_m'}{\epsilon_r} \tag{AI 21}$$

$$\epsilon_\infty = \epsilon_a \frac{B}{D} \tag{AI 22}$$

$$T_{av} = \frac{F}{2C} = \frac{\epsilon_r}{2}\left(\frac{\epsilon_i}{\kappa_i} + \frac{\epsilon_a}{\kappa_a}\right) + \frac{RC_m'}{2\kappa_a}\left[\frac{1 - p}{2 + p} + \frac{\kappa_a}{\kappa_i'}\right]. \tag{AI 23}$$

The individual magnitudes of each dispersion term

$$\Delta\kappa_1 = \kappa_{1\infty} - \kappa_{10}\,; \qquad \Delta\kappa_2 = \kappa_{2\infty} - \kappa_{20} \tag{AI 24}$$

$$\Delta\epsilon_1 = \epsilon_{10} - \epsilon_{1\infty}\,; \qquad \Delta\epsilon_2 = \epsilon_{20} - \epsilon_{2\infty} \tag{AI 25}$$

can be calculated from the total dispersion magnitudes

$$\Delta\kappa = \Delta\kappa_1 + \Delta\kappa_2 \tag{AI 26}$$

$$\Delta\epsilon = \Delta\epsilon_1 + \Delta\epsilon_2 \tag{AI 27}$$

and the time constants T_1 and T_2 as follows. From Equations AI 12 *a*, AI 13 *a*

$$\frac{\Delta\kappa}{\epsilon_r} = \frac{\Delta\epsilon_1}{T_1} + \frac{\Delta\epsilon_2}{T_2}. \tag{AI 28}$$

Combining Equations AI 27 and AI 28

$$\Delta\epsilon - T_1\frac{\Delta\kappa}{\epsilon_r} = \Delta\epsilon_2\left(1 - \frac{T_1}{T_2}\right) \tag{AI 29}$$

$$\Delta\epsilon - T_2\frac{\Delta\kappa}{\epsilon_r} = \Delta\epsilon_1\left(1 - \frac{T_2}{T_1}\right). \tag{AI 30}$$

From $\Delta\epsilon_1$ and $\Delta\epsilon_2$ the magnitudes $\Delta\kappa_1$ and $\Delta\kappa_2$ are calculated using Equations AI 12 *a* and AI 13 *a*.

APPENDIX II

A simpler expression for the high frequency limit dielectric constant ϵ_∞ than given in Equation AI 22 of Appendix I can be derived. The following two equations apply

$$\frac{K - K_a}{K + 2K_a} = P\frac{K_p - K_a}{K_p + 2K_a} \tag{AII 1}$$

$$\frac{K_p - K_m}{K_p + 2K_m} = \left(\frac{R - d}{R}\right)^3\frac{K_i - K_m}{K_i + 2K_m}. \tag{AII 2}$$

The subscripts p, m, i, and a denote effective ("equivalent homogeneous") particle, membrane particle, and interior and suspending phase. R is the radius of the particle, d the membrane thickness, and p the volume fraction occupied by the particles. The equations are valid for complex specific admittances $K = \kappa + j\omega\epsilon\epsilon_r$. They have been given first by Maxwell (18) for real conductivities, but can be generalized to the complex case since the boundary conditions of the problem can be identically stated for the DC and AC case.

For very high frequencies the complex specific admittances K reduce to dielectric constants. Rewriting Equation 2

$$\epsilon_p = \epsilon_m\frac{1 + 2a\dfrac{\epsilon_i - \epsilon_m}{\epsilon_i + 2\epsilon_m}}{1 - a\dfrac{\epsilon_i - \epsilon_m}{\epsilon_i + 2\epsilon_m}}. \tag{AII 3}$$

Equation AII 1 states for small p

$$\epsilon = \epsilon_a\left[1 + 3p\frac{\epsilon_p - \epsilon_a}{\epsilon_p + 2\epsilon_a}\right]. \tag{AII 4}$$

Thus the dielectric change

$$\Delta\epsilon = \epsilon - \epsilon_a = 3p\epsilon_a\frac{\epsilon_p - \epsilon_a}{\epsilon_p + 2\epsilon_a} \tag{AII 5}$$

and the dielectric increment

$$\frac{\Delta\epsilon}{100p} = 2.4\,\frac{\epsilon_p - \epsilon_a}{\epsilon_p + 2\epsilon_a} \qquad \text{(AII 6)}$$

using $\epsilon_a = 82$. The increment varies for the range $\epsilon_p \ll \epsilon_a$ to $\epsilon_p \gg \epsilon_a$ between -1.2 and $+2.4$.

In the case of present interest $a = 0.3$, $\epsilon_i = 82$ and $\epsilon_m = 11$, Equation AII 3 gives $\epsilon_p = 20$. If $\epsilon_m = 30$ then $\epsilon_p = 41$. For these ϵ_p values

$$\frac{\Delta\epsilon}{100p} = -0.48 \quad \text{for} \quad \epsilon_m = 30$$

$$= -1.07 \quad \text{for} \quad \epsilon_m = 3. \qquad \text{(AII 7)}$$

These expressions may be used to calculate $\Delta\epsilon$ and ϵ_∞ from ϵ_m or conversely, provide an estimate of ϵ_m from $\Delta\epsilon$. In Fig. 4 $\Delta\epsilon$ is plotted against p for both cases $\epsilon_m = 11$ and $\epsilon_m = 3$.

REFERENCES

1. Stoeckenius, W., and D. M. Engelman. 1969. *J. Cell Biol.* **42**:613.
2. Miyamoto, V. K., G. W. Pohl, and W. Stoeckenius. 1969. *Biophys. J.* **9**:A-175.
3. Miyamoto, V. K., and W. Stoeckenius. 1970. *Biophys. J.* **10**:140a.
4. Schwan, H. P. 1957. *In* Advances in Biological and Medical Physics. J. H. Lawrence and C. A. Tobias, editors. Academic Press, Inc., New York. **5**:147.
5. Schwan, H. P., and H. J. Morowitz. 1962. *Biophys. J.* **2**:395.
6. Schwan, H. P., G. Schwarz, J. Maczuk, and H. Pauly. 1962. *J. Phys. Chem.* **66**:2626.
7. Schwarz, G. 1962. *J. Phys. Chem.* **66**:2636.
8. Bartlett, G. R. 1959. *J. Biol. Chem.* **234**:466.
9. Folch, J., M. Lees, and G. H. Stanley. 1957. *J. Biol. Chem.* **226**:497.
10. Pauly, H., L. Packer, and H. P. Schwan. 1960. *J. Biophys. Biochem. Cytol.* **7**:589.
11. Schwan, H. P., and K. Sittel. 1953. *Trans. Amer. Inst. Elec. Eng. Part I.* 114.
12. Schwan, H. P. 1963. *In* Physical Techniques in Biological Research. W. L. Nastuk, editor. Academic Press, Inc., New York. **6**:323.
13. Schwan, H. P. 1965. *Ann. N. Y. Acad. Sci.* **125**:344.
14. Pennock, B. E., and H. P. Schwan. 1969. *J. Phys. Chem.* **73**:2600.
15. Oldenburg, John T. 1970. A theoretical analysis of dielectric measurements as applied to the determination of the electrical properties of a system of artificial vesicular membranes. Masters Thesis. University of Pennsylvania, Philadelphia.
16. Pauly, H., and H. P. Schwan. 1966. *Biophys. J.* **6**:621.
17. Pauly, H., and H. P. Schwan. 1959. *Z. Naturforsch.* **14b**:125.
18. Maxwell, J. C. 1873. A Treatise of Electricity and Magnetism. The Oxford University Press, London.